Binary Glass-Forming Materials: Mixtures of Sorbitol and Glycerol†

Kalyan Duvvuri and Ranko Richert*

Department of Chemistry and Biochemistry, Arizona State University, Tempe, Arizona 85287-1604

Received: December 31, 2003; In Final Form: March 3, 2004

The dynamics of sorbitol/glycerol mixtures across the entire composition range has been characterized by dielectric relaxation measurements for frequencies between 10 mHz and 10 MHz. We explore the gradual change in the glass transition temperature (T_g), fragility (m), nonexponentiality (β_{KWW}), and occurrence of a secondary Johari−Goldstein type relaxation as a function of the mole fraction. Regarding the crystallization tendency at room temperature and the freezing of molecular motion below T_g, these mixtures differ qualitatively from aqueous solutions of sugars or other polyols.

1. Introduction

Amorphous solids and viscous liquids play an important role in various technological applications and areas of fundamental science. Materials like obsidian, window glass, polymers, amorphous metals, and many food products feature particular properties which originate from the disordered nature of the molecular arrangements in these systems. For the majority of liquids, crystallization prohibits the formation of a viscous supercooled state below the melting temperature T_m. In the case of glass-forming systems, however, crystallization can be avoided easily and the liquid character is retained in the temperature range between T_m and the glass transition temperature T_g. At T_g a purely kinetic transition into the glassy state occurs upon cooling, where the time required for relaxing the structure of the system begins to exceed a time window set by experimental conditions, typically 100 s. Cooling a viscous melt below its glass transition temperature T_g is the most typical approach to vitreous solids, but other pathways to the solid state exist as well, for example, the isothermal increase of viscosity by solvent evaporation or polymerization reactions.

Glass-forming liquids are still challenging regarding a satisfactory understanding of the rich phenomenology of these complex systems.[1] In the viscous regime, $T_g \leq T \leq T_m$, the structural or α-relaxation time varies more than 10 orders of magnitude. In this supercooled state of a liquid, non-Arrhenius temperature dependences and nonexponential relaxation patterns appear to be the rule rather than the exception.[2−4] The temperature dependence of some characteristic relaxation time τ is often well approximated by the Vogel−Fulcher−Tammann (VFT) equation[5]

$$\log_{10}(\tau/s) = A + B/(T - T_0) \qquad (1)$$

implying a divergence of τ if extrapolated to a finite temperature $T = T_0$, unless $T_0 = 0$ restores the Arrhenius case. A convenient parameter for quantifying the extent of the deviation from an Arrhenius type behavior is the fragility index[6,7]

$$m = \left.\frac{\mathrm{d}\log_{10}\langle\tau/s\rangle}{\mathrm{d}(T_g/T)}\right|_{T=Tg} \qquad (2)$$

equivalent to the slope in a fragility plot, $\log\langle\tau/s\rangle$ versus T_g/T, at $T = T_g$.[8] Simple activation or Arrhenius behavior is equivalent to the limit of "strong" liquids with $m = 16$, while the most fragile molecular liquids exhibit values as high as $m = 156$.[9] Fragile liquids are typically those which show a pronounced secondary or β-relaxation of the Johari−Goldstein type,[10−13] although exceptions from this rule do exist.[14] On this fragility scale, the two pure compounds considered here differ considerably: Glycerol has $m = 53$ without a trace of a β-process, while sorbitol is very fragile with $m = 127$ and associated with a β-process of remarkable intensity.

In many cases, the glassy state of matter is used as host material for some functional guest molecules. Dielectric studies of such probe dynamics have been pioneered by Williams.[15,16] Unlike their polycrystalline counterparts, amorphous solids and melts are optically transparent and thereby facilitate a number of optical experiments on molecules embedded in the glass matrix. Optical hole-burning,[17] spectral diffusion,[18] and single molecule[19] spectroscopy are examples for experiments involving amorphous solids. A more recent application of glass-forming materials is the use of noncrystallizing liquids for freezing the structure of proteins in their natural and functional state. Because many biological molecules require protic environments like water, cooling such systems requires a cryoprotectant, that is, a liquid with a strongly suppressed crystallization tendency compared with water.

Well-investigated binary organic glass-formers are aqueous sugar solutions or otherwise plasticized carbohydrates.[20−26] Such binary systems exhibit either good glass-formation ability or at least a strongly reduced tendency to crystallize compared with pure water. Here we explore the properties of binary mixtures of two polyols, glycerol and sorbitol, whose structures are shown in Chart 1. These are chemically very similar liquids but with significantly different behavior regarding the relaxation behavior and glass formation of the pure compounds. Our study focuses on the dynamics of sorbitol/glycerol mixtures across the entire composition range as probed by dielectric relaxation measurements. Temperature and composition dependent relaxation times indicate how T_g, fragility, nonexponentiality, and the appearance of a secondary relaxation peak change with the composition. Because of the similar chemical nature of the two components, sorbitol and glycerol, we hope to be able to adjust the physical properties of the liquid and glass without a significant change of the chemistry of the system.

† Part of the special issue "Gerald Small Festschrift".

10.1021/jp031366b CCC: $27.50
Published on Web 04/23/2004

CHART 1: Chemical Structures of D-Sorbitol ($C_6H_{14}O_6$) and Glycerol ($C_3H_8O_3$)

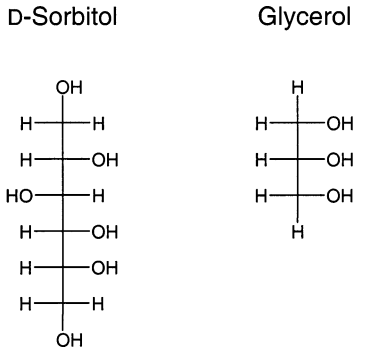

2. Experimental Section

The compounds D-sorbitol (98%) and glycerol (99%+, anhydrous) have both been purchased from Aldrich and are used as received. Sorbitol is heated sufficiently above its melting point in order to obtain a clear liquid and then mixed with the appropriate amount of glycerol as determined by weight. The neat liquids obtained in this manner reproduce literature dielectric data, indicating that chemical degradation is not an issue. The liquid mixture is held between two brass electrodes which are separated by thin Teflon stripes arranged in a radial geometry. The dimensions of this capacitor with 20 mm diameter and 50 μm thickness result in a geometric capacity of $C_0 = 55.6$ pF. All samples are measured inside a nitrogen-gas cryostat where the temperature is stabilized and measured by a Novocontrol Quatro controller. The stability of the temperature reading is better than 0.05 K.

Frequency dependent impedance measurements were performed using a Solatron 1260 gain-phase-analyzer equipped with a Mestec DM-1360 transimpedance amplifier. Data are acquired for frequencies in the range 10 mHz $\leq f \leq$ 10 MHz, with the frequencies being logarithmically spaced at a density of 8 per decade. This impedance technique requires a reference measurement in order to calibrate the frequency dependent transimpedance $Z_t(\omega)$ of the DM-1360. For the present case, the empty sample capacitor turned out to be appropriate.

Like sorbitol, the dielectric loss curves of many sugars and polyalcohols are indicative of three distinct features: the dc conductivity, a primary relaxation peak, and a secondary relaxation peak. In order to quantify the characteristics of these processes as a function of composition and temperature, we follow common practice and subject the susceptibility data to the following empirical fit function:

$$\epsilon^*(\omega) = \epsilon_\infty + \frac{\Delta\epsilon_1}{[1 + (i\omega\tau_1)^{\alpha_1}]^{\gamma_1}} + \frac{\Delta\epsilon_2}{1 + (i\omega\tau_2)^{\alpha_2}} - i\frac{\sigma_{dc}}{\epsilon_0\omega} \quad (3)$$

where ϵ_∞ is the dielectric constant in the high-frequency limit and $\Delta\epsilon_i$ is the relaxation strength of a particular process. The second term of this equation represents a Havriliak−Negami[27] (HN) function used to reflect the asymmetrically broadened profiles of the primary (α) process, with α and γ respectively characterizing the symmetric and asymmetric broadening. The secondary (β) relaxation is usually well described by the symmetric Cole−Cole (CC) function, justifying the third term in eq 3. Finally, the dc conductivity is quantified by the parameter σ_{dc}. Identifying the dielectric relaxation with the sum of the HN and CC peaks implies the independence of the α- and β-processes. While this is justified for situations in which the two profiles show only little overlap, the reliability of the parameters in the merging regime of the α- and β-relaxation is bound to be limited.[28]

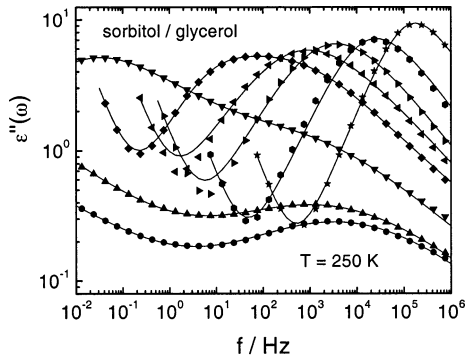

Figure 1. Dielectric properties of sorbitol/glycerol mixtures at a common temperature of $T = 250$ K, shown in terms of the loss $\epsilon''(\omega)$ vs frequency. The sorbitol mole fraction x_S ranges from 0 to 0.82 in the order from low to high peak frequency regarding the primary relaxation. For clarity, only every other point is shown and the low-frequency conductivity contributions are partly omitted. See Table 1 for symbol and composition identification.

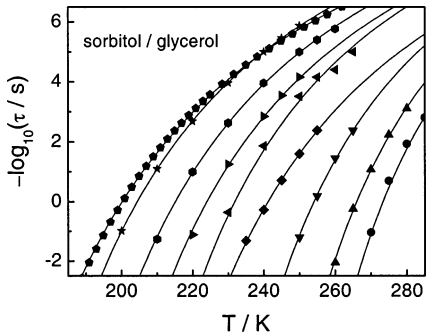

Figure 2. Temperature dependence of the primary dielectric relaxation time, τ_1 in eq 3, for sorbitol/glycerol mixtures of various compositions. Symbols represent experimental data, solid lines are for the VFT fits of eq 1 with a common prefactor, $A = -15$, and values for B and T_0 compiled in Table 1. The sorbitol mole fraction x_S ranges from 0 to 1 in the order from right to left curves. Data for the secondary relaxations are omitted in this graph. See Table 1 for symbol and composition identification.

3. Results

Dielectric relaxation data are acquired for temperatures between 190 and 280 K for seven different mole fractions x_S of sorbitol in glycerol. Frequency dependent curves for the dielectric loss $\epsilon''(\omega)$ at a common temperature of $T = 250$ K are compiled in Figure 1 for the compositions listed in Table 1. The frequency resolved dielectric loss data $\epsilon''(\omega)$ were subject to fit procedures using eq 3. The typical coincidence between fit and data can be seen for the $T = 250$ K data in Figure 1. The characteristic relaxation times $\tau_\alpha = \tau_1$ for the primary process obtained in this manner are compiled graphically as symbols in Figure 2 as $-\log(\tau)$ versus T. For compositions with a sorbitol weight percentage above 70% or a mole fraction $x_S \geq 0.54$, a secondary process is clearly identified as a further loss peak. For these samples, both primary (α, τ_1) and secondary (β, τ_2) relaxation times are shown in an activation plot, $-\log(\tau)$ versus $1/T$, in Figure 3.

The relaxation time data in Figure 2 has been analyzed on the basis of the VFT dependence, eq 2. The preexponential factor A has been kept constant at $A = -15$ for all values of x_S. The results for B and T_0 derived from these VFT fits are compiled in Table 1, and the actual fit curves are included as lines in Figure 2.

TABLE 1: Characteristic Parameters of the Sorbitol/Glycerol Mixtures as a Function of Composition: Mole Fraction x_S, Peak (α or β) and Symbol Identification, Glass Transition Temperature T_g, Fragility m, Stretching Exponent β_{KWW} at $T \approx T_g$, and VFT Fit Values A, B, and T_0

sorbitol wt %	x_S	symbol	T_g / K	m	β_{KWW}	A	B / K	T_0 / K
100	1.00	α: ●	267.5	127	0.37	−15	748	223.5
90	0.82	α: ▲	259.8	95	0.38	−15	791	213.3
80	0.67	α: ▼	247.2	82	0.33	−15	871	196.0
70	0.54	α: ◆	232.5	61	0.34	−15	1107	167.4
60	0.43	α: ◀	224.5	69	0.28	−15	943	169.0
50	0.34	α: ▶	215.9	61	0.23	−15	1031	155.3
40	0.25	α: ⬢	206.9	57	0.39	−15	1055	144.8
20	0.11	α: ★	196.1	53	0.52	−15	1067	133.3
0	0.00	α: ⬟	190.8	53	0.65	−15	1200	120.2
100	1.00	β: ○	-	-	-	−13.8	2300	0
90	0.82	β: △	-	-	-	−18.8	3680	0
80	0.67	β: ▽	-	-	-	−22.3	4670	0
70	0.54	β: ◇	-	-	-	-	-	-

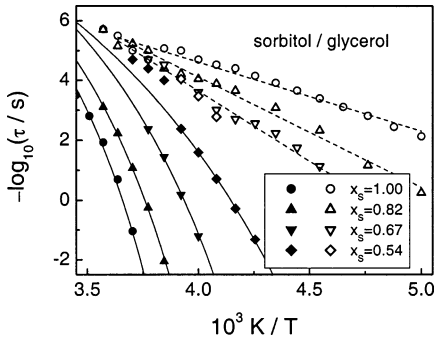

Figure 3. Activation map for the primary (solid symbols) and secondary (open symbols) dielectric relaxation times, τ_1 and τ_2 in eq 3, for sorbitol/glycerol mixtures of those compositions for which β-processes are detected. Symbols represent experimental data, solid lines are for the VFT fits of eq 1 with $A = -15$ and values for B and T_0 compiled in Table 1, dashed lines are for Arrhenius fits (eq 1 with $T_0 = 0$) with the values for A and B compiled in Table 1. The inset identifies the symbols for the various sorbitol mole fractions x_S.

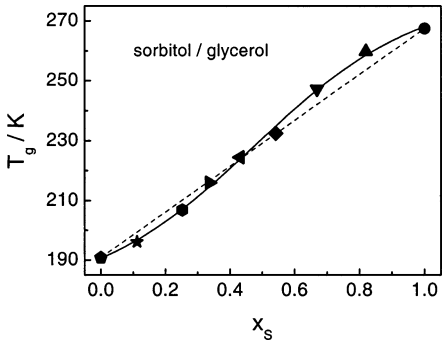

Figure 4. Dependence of the glass transition temperature T_g on composition x_S for the sorbitol/glycerol mixtures, where x_S is the mole fraction of sorbitol. The dashed line represents the linear relation of eq 4, the solid line serves as a guide only.

4. Discussion

Both glass-forming liquids of present interest, glycerol and sorbitol, have been investigated earlier with regards to their dynamics. Glycerol has been the focus of many studies targeted at the relaxation behavior of molecular supercooled systems because it is an excellent glass-former with a large dipole moment and virtually no tendency to crystallize.[29−35] Sorbitol has received significant attention due to its pronounced secondary or slow β-relaxation of the Johari−Goldstein type.[12,36−43] Of particular interest for the present work are also those cases where the homologous series $C_nH_{2n+2}O_n$ of polyols, glycerol ($n = 3$), threitol ($n = 4$), xylitol ($n = 5$), and sorbitol ($n = 6$), has been addressed in a systematic fashion.[44−46] This series exhibits a gradual variation from a moderately fragile ($m = 53$) and nonexponentially relaxing ($\beta_{KWW} = 0.65$) liquid with no obvious β-relaxation (glycerol) to a very fragile ($m = 127$) liquid with a wide distribution of relaxation times ($\beta_{KWW} = 0.37$) and with an intense dielectric β-peak. The two liquids also differ considerably in their glass transition temperatures, $T_g = 191$ K for glycerol versus $T_g = 268$ K for sorbitol. In order to assess the dynamics for the mixtures, the relaxation time data for each concentration has been subject to a VFT fit using eq 1 with the constraint of a composition invariant preexponential factor $A = -15$. The resulting parameters are compiled in Table 1, and the fit curves are included as solid lines in Figure 2 and Figure 3.

Based upon the chemical similarity of the two compounds, it is not surprising that the present two polyols are miscible across the entire composition range and that there are no signs of a phase separation in terms of two distinct glass transitions at any concentration. As shown in Figure 4, the value of $T_g(x_S)$ for the mixture varies practically linearly with the sorbitol mole fraction x_S. These glass transition temperatures are derived from the VFT fit parameters using $T_g = T_0 + B/(2 - A)$. A straight line connecting the limiting points at $x_S = 0$ and $x_S = 1$

$$T_g(x_S) = 190.8\ \text{K} + x_S(76.7\ \text{K}) \qquad (4)$$

reproduces the observed values within approximately 2% (dashed line in Figure 4). These results show that composition can tune the glass transition to some desired value within a range of approximately 80 K. However, the value of T_g captures only one aspect of the entire behavior regarding the dynamics of molecules by identifying the temperature at which the relaxation time has reached a value of $\tau_g = \tau(T_g) = 100$ s.

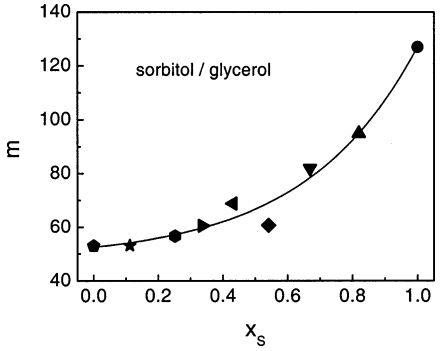

Figure 5. Dependence of the fragility parameter m on composition x_S for the sorbitol/glycerol mixtures, where x_S is the mole fraction of sorbitol. The definition of m is given in eq 2. The line serves as a guide only.

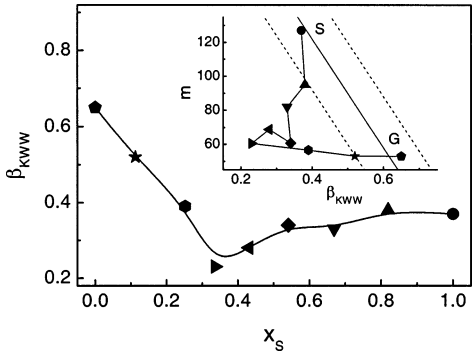

Figure 6. Dependence of the stretching exponent β_{KWW} for the primary process on composition x_S for the sorbitol/glycerol mixtures, where x_S is the mole fraction of sorbitol. The line serves as a guide only. Inset: Relation between fragility m and exponent β_{KWW} for various compositions from pure sorbitol (S) to pure glycerol (G). The straight lines indicate the typical correlation range for pure materials, $m = 250(\pm 30) - 320\times\beta_{KWW}$, taken from ref 6.

Glass-forming liquids differ in their rate at which the relaxation time increases as the system is cooled toward the glass transition. There are various ways to quantify this extent to which the temperature dependence of the relaxation time deviates from simple Arrhenius behavior. The most widely used is the classification in terms of the strong−fragile pattern suggested by Angell, which is based upon scaling the relaxation time or viscosity data as log (τ/s) versus T_g/T.[8] For materials which exhibit a pronounced β-relaxation, the fragility index m defined in eq 2 as the slope of a fragility curve at T_g is a reliable measure because the α- and β-peaks are well separated on the frequency scale for temperatures near T_g. Because the present VFT fits shown in Figure 2 reflect the observed relaxation times near T_g to a good degree of accuracy, the VFT parameters of Table 1 are used in order to determine the fragility indices m according to

$$m = \frac{BT_g}{(T_g - T_0)^2} = 2 - A + \frac{T_0}{B}(2 - A)^2 \qquad (5)$$

The variation of m with composition is included in Table 1 and shown graphically in Figure 5. According to these results, adding sorbitol up to a mole fraction of $x_S = 0.5$ has little effect on the fragility, while the effect of adding sorbitol in the range $x_S >$ 0.5 accounts for most of the total increase in fragility.

One of the characteristic features of supercooled liquids is the correlation between the fragility and the width of the distribution of relaxation times.[6] For correlation functions which are measured in the time domain, the deviations from a purely exponential pattern with a single relaxation time are typically observed as a relaxation of the Kohlrausch−Williams−Watts (KWW) type[47,48]

$$\phi(t) = \phi_0 \exp[-(t/\tau_{KWW})^{\beta_{KWW}}] \qquad (6)$$

with a stretching exponent β_{KWW} below unity. For a large number of pure glass-forming liquids, $m = 250(\pm 30) - 320\times$-($\beta_{KWW}$) has been observed, that is, strong deviations from an Arrhenius-like temperature dependence are associated with a strong departure from exponential dynamics.[6]

In order to assess this correlation for the present series of sorbitol/glycerol mixtures, we have numerically generated the time-domain equivalents of the HN type relaxations from the shape parameters α_1 and γ_1 in eq 3. Fitting the resulting decays with eq 6 leads to the β_{KWW} values listed in Table 1 and plotted in Figure 6. This graph shows that the bulk of the relaxation time dispersion increase occurs in the initial 40% mole fraction range of adding sorbitol to glycerol, while β_{KWW} changes only little for x_S above 0.5. The inset of Figure 6 shows how m relates to β_{KWW} for the various concentrations of the present binary system. The straight lines in this plot represent the correlation range observed for pure supercooled liquids, and it is obvious that the mixture fails to follow this trend. Instead, β_{KWW} changes mainly in the glycerol rich part, $x_S \leq 0.5$, while the remainder of the composition range affects more the fragility index m. The departure from the trend seen for pure substances is assumed to originate from concentration fluctuations, which are a source of additional relaxation time dispersion without necessarily affecting the fragility accordingly. Therefore, this "rectangular" motion within the $m-\beta_{KWW}$ plane is not the expected behavior for the homologous series of neat polyols studied earlier.[44] According to the inset of Figure 6, the concentration fluctuations appear to be most effective at a concentration around $x_S \approx {}^1/_3$, equivalent to 50% weight fraction.

We now turn to the Johari−Goldstein slow β-relaxation seen in a number of glass-forming liquids.[10] The characteristic features of this process are the occurrence in the vitreous state below T_g, the Arrhenius temperature dependence of the average relaxation time, wide and symmetric dielectric loss peaks, amplitudes that increase with increasing temperature, and the merging with the primary relaxation where the time constants reach a value of $\tau_B = 10^{-7}$ s.[11,12,49] This secondary process is observed mainly in liquids of considerable fragility, like sorbitol,[12,37−39] whereas its existence in less fragile systems like glycerol is all but obvious.[50,51] However, aging experiments[52] and a scrutiny in terms of the coupling model[14] indicate that the "excess" loss within the high-frequency wing of those cases without a clear-cut β-peak should be interpreted as a Johari−Goldstein process which remains hidden below the signal of the α-process. In support of this notion, the study of Döss et al.[44] demonstrates the gradual change from a pronounced β-process to a wing-type glass-former for the homologous series of neat polyols: glycerol, threitol, xylitol, sorbitol.

According to the analysis of loss spectra for the sorbitol/glycerol mixtures, Johari−Goldstein type peaks are being observed only for sorbitol mole fractions in excess of $x_S = 0.54$. As seen in Figure 3, the activation energies change considerably with sorbitol concentration, and an extrapolation of this trend predicts the absence of a distinct β-peak for the glycerol rich mixtures with $x_S < 0.54$. Indeed, we observe that the cases of $x_S < 0.54$ display broadened loss profiles, but without an

obvious indication of a secondary relaxation process. Therefore, the present findings suggest that the gradual transition from presence to absence of the slow secondary process occurs as an approach of α- and β-peak on the frequency scale instead of a simple loss of β-relaxation amplitude. Because the peak dielectric loss of the primary process usually exceeds that of the secondary one, a separation of 2 or 3 decades in frequency is required for the Johari−Goldstein relaxation to appear as additional peak in the dielectric loss curves. With increasing sorbitol concentration, the β-relaxation appears in the present measurements as soon as the fragility exceeds values around $m = 80$. On the basis of the average $\beta_{KWW}-m$ correlation established by Böhmer et al.,[6] $\beta_{KWW} = (250 - m)/320$, stretching exponents of $\beta_{KWW} \leq 0.5$ are required for a clearly measurable β-peak. At least qualitatively, this is entirely consistent with previous assessments of the β-relaxation appearance in terms of the coupling parameter $n = 1 - \beta_{KWW}$.[14,53] As a result of the inevitable concentration fluctuations in binary systems, the required dispersion inherent in the above inequality, $\beta_{KWW} \leq 0.5$, will not be reflected in the present $\beta_{KWW}(x_S)$ values of the mixtures.

5. Conclusions

We have studied the structural relaxation of supercooled sorbitol/glycerol mixtures regarding the peak relaxation time, width of the relaxation time distribution, fragility, and behavior of the Johari−Goldstein β-relaxation. While the glass transition varies nearly linearly between 191 and 268 K with the sorbitol mole fraction x_S, the changes of the nonexponentiality (β_{KWW}) and the fragility (m) are most pronounced in the respective ranges $0 \leq x_S \leq 0.5$ and $0.5 \leq x_S \leq 1$. Due to the concentration fluctuations inherent in binary systems, the relaxation time distribution displays a maximum (minimum in β_{KWW}) near $x_S = {}^1/_3$ and the mixture fails to follow the typical $m-\beta_{KWW}$ correlation observed for pure glass-formers.

Regarding the occurrence of a slow β-relaxation, fragility appears to be a decisive factor. Similar to the trends reported for pure systems, a secondary process appears as a distinct dielectric loss peak when the fragility exceeds values around $m = 80$, equivalent to $x_S > {}^2/_3$ for the present mixtures. With increasing glycerol concentration, the β-peak gradually approaches the peak frequency of the α-process and eventually disappears in the high-frequency wing of the primary relaxation feature. Therefore, the mixture shows a gradual change from a supercooled liquid which exhibits a separate β-peak to one which displays the typical high-frequency wing only. This observation lends further support to the picture that a β-relaxation in less fragile systems does exist but its most probable relaxation frequency is not sufficiently separated from the larger main peak in order to give rise to a distinct feature within the loss spectrum.

Finally, we point out two advantages of using glycerol instead of water for plasticizing polyols (or sugars) with the aim of combining the glass-formation capability of viscous protic materials (like sorbitol) with lower glass transitions and thus higher room temperature fluidity. Because glycerol is glass-forming as a pure liquid and relatively viscous already at room temperature, the crystallization tendency of such mixtures using glycerol is less pronounced than those involving water. In contrast to glycerol, the addition of water to polyols greatly increases the amplitude of the secondary process. As a result, the dielectric signature of the main relaxation process and thus the value for T_g becomes difficult to identify in the case of aqueous solutions of sugars. Moreover, a secondary relaxation with considerable amplitude implies that the glassy state below T_g remains associated with a relatively high molecular mobility on the microscopic level. If such glasses are intended to immobilize guest molecules, sub-T_g relaxations are not desirable.

References and Notes

(1) Angell, C. A.; Ngai, K. L.; McKenna, G. B.; McMillan, P. F.; Martin, S. W. *J. Appl. Phys.* **2000**, *88*, 3113.
(2) Ediger, M. D.; Angell, C. A.; Nagel, S. R. *J. Phys. Chem.* **1996**, *100*, 13200.
(3) Ediger, M. D. *Annu. Rev. Phys. Chem.* **2000**, *51*, 99.
(4) Richert, R. *J. Phys.: Condens. Matter* **2002**, *14*, R703.
(5) (a) Vogel, H. *Phys. Z.* **1921**, *22*, 645. (b) Fulcher, G. S. *J. Am. Ceram. Soc.* **1923**, *8*, 339. (c) Tammann, G.; Hesse, W. *Z. Anorg. Allg. Chem.* **1926**, *156*, 245.
(6) Böhmer, R.; Ngai, K. L.; Angell, C. A.; Plazek, D. J. *J. Chem. Phys.* **1993**, *99*, 4201.
(7) Böhmer, R.; Angell, C. A. In *Disorder Effects on Relaxational Processes*; Richert, R., Blumen, A., Eds.; Springer: Berlin, 1994.
(8) Angell, C. A. *J. Non-Cryst. Solids* **1991**, *131−133*, 15.
(9) Richert, R.; Duvvuri, K.; Duong, L.-T. *J. Chem. Phys.* **2003**, *118*, 1828.
(10) Johari, G. P.; Goldstein, M. *J. Chem. Phys.* **1970**, *53*, 2372; **1971**, *55*, 4245.
(11) Kudlik, A.; Tschirwitz, C.; Benkhof, S.; Blochowicz, T.; Rössler, E. *Europhys. Lett.* **1997**, *40*, 649.
(12) Wagner, H.; Richert, R. *J. Phys. Chem. B* **1999**, *103*, 4071.
(13) Ngai, K. L.; M. Paluch *J. Chem. Phys.* **2004**, *120*, 857.
(14) Ngai, K. L.; Lunkenheimer, P.; Leon, C.; Schneider, U.; Brand, R.; Loidl, A. *J. Chem. Phys.* **2001**, *115*, 1405.
(15) Williams, G.; Hains, P. H. *Chem. Phys. Lett.* **1971**, *10*, 585.
(16) Williams, G. *Chem. Rev.* **1972**, *72*, 55.
(17) Reinot, T.; Zazubovich, V.; Hayes, J. M.; Small, G. J. *J. Phys. Chem. B* **2001**, *105*, 5083.
(18) Schlichter, J.; Friedrich, J.; Herenyi, L.; Fidy, J. *Biophys. J.* **2001**, *80*, 2011.
(19) Dickson, R. M.; Norris, D. J.; Tzeng, Y.-L.; Moerner, W. E. *Science* **1996**, *274*, 966.
(20) Moran, G. R.; Jeffrey, K. R.; Thomas, J. M.; Stevens, J. R. *Carbohydr. Res.* **2000**, *328*, 573.
(21) Orford, P. D.; Parker, R.; Ring, S. G. *Carbohydr. Res.* **1990**, *196*, 11.
(22) Lourdin, D.; Ring, S. G.; Colonna, P. *Carbohydr. Res.* **1998**, *306*, 551.
(23) Höchtl, P.; Boresch, S.; Steinhauser, O. *J. Chem. Phys.* **2000**, *112*, 9810.
(24) Nozaki, R.; Zenitani, H.; Minoguchi, A.; Kitai, K. *J. Non-Cryst. Solids* **2002**, *307−310*, 349.
(25) Murthy, S. S. N. *J. Phys. Chem. B* **2000**, *104*, 6955.
(26) Sudo, S.; Shinyashiki, N.; Yagihara, S. *J. Mol. Liq.* **2001**, *90*, 113.
(27) Havriliak, S.; Negami, S. *Polymer* **1967**, *8*, 161.
(28) Ngai, K. L. *J. Phys.: Condens. Matter* **2003**, *15*, S1107.
(29) Dixon, P. K.; Nagel, S. R.; Weitz, D. A. *J. Chem. Phys.* **1991**, *94*, 6924.
(30) Wuttke, J.; Chang, I.; Fujara, F.; Petry, W. *Physica B* **1997**, *234−236*, 431.
(31) Schröter, K.; Donth, E. *J. Chem. Phys.* **2000**, *113*, 9101.
(32) Ryabov, Ya. E.; Hayashi, Y.; Gutina, A.; Feldman, Y. *Phys. Rev. B* **2003**, *67*, 132202.
(33) Lunkenheimer, P.; Pimenov, A.; Dressel, M.; Goncharov, Yu. G.; Böhmer, R.; Loidl, A. *Phys. Rev. Lett.* **1996**, *77*, 318.
(34) Duvvuri, K.; Richert, R. *J. Chem. Phys.* **2003**, *118*, 1356.
(35) Jeffrey, K. R.; Richert, R.; Duvvuri, K. *J. Chem. Phys.* **2003**, *119*, 6150.
(36) Angell, C. A.; Smith, D. L. *J. Phys. Chem.* **1982**, *86* (6), 3845.
(37) Nozaki, R.; Suzuki, D.; Ozawa, S.; Shiozaki, Y. *J. Non-Cryst. Solids* **1998**, *235−237*, 393.
(38) Olsen, N. B. *J. Non-Cryst. Solids* **1998**, *235−237*, 399.
(39) Power, G.; Johari, G. P.; Vij, J. K. *J. Chem. Phys.* **2003**, *119*, 435.
(40) Faivre, A.; Niquet, G.; Maglione, M.; Fornazero, J.; Jal, J. F.; David, L. *Eur. Phys. J. B* **1999**, *10*, 277.
(41) Qiu, X.-H.; Ediger, M. D. *J. Phys. Chem. B* **2003**, *107*, 459.
(42) Wagner, H.; Richert, R. *J. Non-Cryst. Solids* **1998**, *242*, 19.
(43) Richert, R. *Europhys. Lett.* **2001**, *54*, 767.
(44) Döss, A.; Paluch, M.; Sillescu, H.; Hinze, G. *Phys. Rev. Lett.* **2002**, *88*, 095701.

(45) Döss, A.; Paluch, M.; Sillescu, H.; Hinze, G. *J. Chem. Phys.* **2002**, *117*, 6582.
(46) Minoguchi, A.; Kitai, K.; Nozaki, R. *Phys. Rev. E* **2003**, *68*, 031501.
(47) Kohlrausch, R. *Poggendorff's Ann. Phys.* **1854**, *91*, 179.
(48) Williams, G.; Watts, D. C. *Trans. Faraday Soc.* **1970**, *66*, 80.
(49) Richert, R.; Angell, C. A. *J. Chem. Phys.* **1998**, *108*, 9016.
(50) Leheny, R. L.; Nagel, S. R. *J. Non-Cryst. Solids* **1998**, *235*−*237*, 278.
(51) Hansen, C.; Richert, R.; Fischer, E. W. *J. Non-Cryst. Solids* **1997**, *215*, 293.
(52) Schneider, U.; Brand, R.; Lunkenheimer, P.; Loidl, A. *Phys. Rev. Lett.* **2000**, *84*, 5560.
(53) Ngai, K. L. *J. Chem. Phys.* **1998**, *109*, 6982.